Food Chemistry: X 15 (2022) 100378

Contents lists available at ScienceDirect

Food Chemistry: X

journal homepage: www.sciencedirect.com/journal/food-chemistry-x

Effect of water-in-oil-in-water (W/O/W) double emulsions to encapsulate nisin on the quality and storage stability of fresh noodles

Songming Luo [a,*,1], Jundong Chen [a,1], Yuanbo Zeng [a], Jianwu Dai [b], Suqing Li [a], Jing Yan [a], Yaowen Liu [a,*]

[a] College of Food Science, Sichuan Agricultural University, Yaan 625014, China
[b] College of Mechanical and Electrical Engineering, Sichuan Agricultural University, Yaan 625014, China

ARTICLE INFO

Keywords:
Rock bean protein
Microcapsules
Noodles

ABSTRACT

Rock-bean protein (RP) was extracted from wild rock beans by ultrasonic treatment and microwave extraction. The RP has a high content of 7S and 11S globulin components and good heat stability. Subsequently, water-oil-water double emulsions were prepared using a water core containing nisin, momordica charantia extract (MCE), and *Lactobacillus plantarum* as functional additives, corn oil as the intermediate wall, and RP/gum arabic (GA) as the outer wall material. For a ratio of corn oil to water of 5:1, the maximum encapsulation efficiency was 28.22%, and RP/GA had good dispersion characteristics, where the smallest average particle size was achieved for a 1:1 ratio. Finally, the microcapsules were used to study the effect of its addition to noodles. The addition of 2 wt% of the microcapsules to low-gluten flour resulted in a dough with suitable rheology, and can extend the shelf life of the fresh noodles prepared using this dough.

1. Introduction

Currently, microencapsulation technology is being applied in many fields, such as food science, chemical engineering, and energy storage (Sun et al., 2021a). Biotin, probiotics, plant extracts, and other active substances are often encapsulated in microcapsules to protect them from the environment and enable their controlled release (Li et al., 2016). Nisin is widely used in the food industry as a preservative because it is particularly effective against gram-positive bacteria. Nisin is the only globally approved food preservative, and is recognized as a safe bacteriostatic agent by the World Health Organization (WHO) and US FDA (Dillon & Board, 1994). A previous study showed that microcapsules prepared by cross-linking negatively charged gum arabic (GA) can effectively protect the activity of nisin (Gong et al., 2018). And MCE has anti-HIV, anti-ulcer, anti-inflammatory, anti-leukemia, anti-microbial, anti-diabetic, anti-tumor and insect control functions (Taylor, 2002).

Probiotics are a current research topic. *Lactobacillus plantarum* is a probiotic bacterium located in the human gastrointestinal tract. It can improve human health by regulating immunity, lowering serum cholesterol levels, treating inflammatory bowel disease, and inhibiting the proliferation of cancer cells and the growth of pathogenic bacteria (Le & Yang, 2018). Sun et al. (2021b) used a hydrogel prepared from whey protein concentrate, pullulan, and trehalose to encapsulate *Lactobacillus plantarum* in microcapsules, which were then freeze dried. The microcapsule structure effectively improved the viability of *Lactobacillus plantarum* during freeze-drying and storage. Nualkaekul, Lenton, Cook, Khutoryanskiy, and Charalampopoulos (2012) used chitosan and sodium alginate to encapsulate *Lactobacillus plantarum* and added the prepared microcapsules to pomegranate juice. Digestion simulations of the gastrointestinal tract showed that the microcapsules can improve the survival rate of cells, allowing the ingested *Lactobacillus plantarum* to survive digestion and work in the intestinal tract. Many wall materials for microcapsules have been evaluated, including natural biopolymers, polysaccharides, and proteins, which are novel carrier materials for food products owing to their biocompatibility and biodegradability (Liu, Sameen, Ahmed, Dai, & Qin, 2021). Owing to their good stability, favorable hydration, gel-forming, and emulsification properties, plant-protein-based microcapsules are used in many applications (Luo et al., 2022). Only a few studies have added plant proteins to noodles. For example, Rani et al. (2019) mixed soybean flour, sorghum flour, and refined wheat flour to prepare multi-grain noodles. The results showed that the nutrition and antioxidant contents of multi-grain noodles

* Corresponding authors.
E-mail addresses: 251148551@qq.com (S. Luo), lyw@my.swjtu.edu.cn (Y. Liu).
[1] These authors contributed equally to the work.

https://doi.org/10.1016/j.fochx.2022.100378
Received 28 April 2022; Received in revised form 11 June 2022; Accepted 22 June 2022
Available online 27 June 2022

increased, the blood-sugar index was reduced, and cooking loss and hardness were significantly improved. Wee, Loud, Tan, and Forde (2019) studied the effect of adding denatured pea protein isolate on the physical and chemical properties of noodles. The results showed that the addition of denatured pea protein effectively binds starch and limits the gelatinization process, and can also reduce in vitro glucose release.

In this study, we extracted proteins from rock beans, which are representative of wild beans and a special product of Dazhou City, Sichuan Province. We then used RP to encapsulate nisin, *Lactobacillus plantarum*, and MCE, and then added the prepared microcapsules to flour to prepare a new type of nutritious noodles. The basic properties of microcapsules and the effect of adding microcapsules to noodles were investigated. This study provides a reference for the development and utilization of rock beans and the development of new noodle products.

2. Materials and methods

2.1. Materials

Rock beans were purchased from the Farmers Commune of Wanyuan City, Dazhou City, Sichuan Province, China. GA was provided by Shandong Jiju Biotechnology Co., Ltd., China. MCE (MC glycosides 40%, brown powder, 80–120 mesh) was purchased from Guangzhou Yixuan Biotechnology Co., Ltd. (China). Nisin (BR, 900 IU/mg) was purchased from Shanghai Yuanye Biotechnology Co., Ltd., China. Freeze-dried *Lactobacillus plantarum* ATCC 8014 was purchased from the Guangdong Microbial Culture Collection Center (GDMCC), Guangdong, China. Corn oil was provided by China Fulinmen Food Marketing Co., Ltd. Span 80 was purchased from Beijing Qingyuan Food Additives Co., Ltd., China. Low-gluten flour was purchased from China Ya'an Zhongxing Food Co., Ltd. All other chemical reagents used in this experiment were of analytical grade.

2.2. RP extraction

Protein extraction was performed based on a previous method (Luo et al., 2022) and modified appropriately. The fresh rock beans were soaked overnight, and then manually peeled and flapped. The beans were placed on a glass plate and then dried at 30 °C for 5–6 h until hard to the touch. The dried beans were crushed three times with a grinder, and screened with a 40-mesh screen to remove the large particles that were not completely crushed to obtain the as-prepared rock-bean powder.

To obtain degreased rock-bean powder, the as-prepared powder was added to a 15×15 cm^2 filter-paper bag (to fill approximately 2/3 of the bag), which was sealed with a stapler, and placed in a Soxhlet extraction device with petroleum ether (60–90 °C) as the extraction agent. The electric heating sleeve was set to 50 V, and degreasing was performed for 10–12 h. After this time, the filter-paper bag was removed and placed at 30 °C for 10 min to completely dry. After drying, degreased rock-bean powder was obtained. Add 1 g rock-bean powder to 50 mL ultra-pure water, stir until fully dispersed, then add 1 mol/L $NaHCO_3$ to it to adjust the pH to 8.0. Ultrasonic extraction was performed using an XH-2008D ultrasonic instrument (Xianghu Development Co., Ltd., Beijing, China) at 45 °C with a power of 50 W for 15 min, followed by microwave extraction at 45 °C with a power of 50 W for 15 min. After cooling, the samples were placed in a refrigerated centrifuge and treated for 15 min at 4000 rpm. A clear liquid was obtained after collection and its pH was adjusted to 3.8 using 1 mol/L citric acid. After further centrifugation of this liquid at 4000 rpm for 10 min, an ivory sample was obtained. The precipitate was obtained and washed twice with ultra-pure water, followed by centrifugation and dialysis. Finally, the samples were frozen in a refrigerator and freeze-dried for 24 h to obtain the RP. The group without ultrasonic and microwave treatment was regarded as the control group. The RP extraction rate ε (%) was calculated by dividing the mass of albumin after extraction by the mass of skim rock-bean powder used for extraction.

$$\varepsilon = m/M \times 100\% \quad (1)$$

where ε is the extraction rate of the RP, m is the total mass of the RP, and M is the mass of the rock bean powder.

2.3. Sodium dodecyl sulfate polyacrylamide gel electrophoresis

The protein profiles of the extracted RP were analyzed using sodium dodecyl sulfate polyacrylamide gel electrophoresis (SDS-PAGE). Appropriate amounts of the extracted RP powder were added to ultra-pure water (preheated to 40 °C), and the solution pH was adjusted to 8.0, followed by stirring in a magnetic water bath agitator at 40 °C to dissolve the RP. Electrophoresis was performed on the extracted RP with a separation gel and concentrated gel with concentrations of 15% and 5%, respectively. While waiting for the concentrated gel to form, 10 μL of the prepared sample solution was removed and added to 5 μL of loading buffer; this mixture was boiled for 2 min to denature the protein. After 30 min, the concentrated gel was formed and the comb was removed. Then, 10 μL of a commercial marker (180 kDa, Beijing Soleibao Technology Co., Ltd.) was added to the second position, and the same volume of the denatured protein sample was added to the last three channels. The electrode buffer contained 0.1% SDS (pH 8.3), 0.384 mol/L glycine, and 0.05 M Tris, and electrophoresis was performed at 120 V for 2 h. After electrophoresis, the gel was carefully removed with a writing brush and placed in a Petri dish. The gel was stained with 1% Coomassie Brilliant Blue R-250 for 4 h, and then a decolorizing agent (methanol:ethanol:distilled water = 1:1:8) was added to obtain a colorless background. Images were obtained with a gel imager for comparison.

2.4. Fourier transform infrared spectroscopy

The group composition of the RP was extracted using Fourier transform infrared (FTIR) spectroscopy (Suzhou Leiden Scientific Instruments Co., Ltd., Suzhou, China) with the tablet method. Each protein-powder sample was tested twice, and 32 scans with a resolution of 4 cm^{-1} were obtained over a wavenumber range of 500–4000 cm^{-1} (Zhang et al., 2021).

2.5. Thermal stability tests

The prepared RP powder (2 mg) was placed in an aluminum crucible (diameter of 5.4 mm and depth of 2.6 mm). The crucible was covered with a cap and placed in the DSC instrument (DSC Q200, V24.2 Build 107). Measurements were performed over a temperature range of 10–200 °C, with a nitrogen gas flow of 30 mL/min. During testing, the sample purge flow was recorded (mL/min). The weight of an empty hermetic pan was used as the reference. The experiment was performed twice, and the best one was chosen for analysis.

2.6. High performance liquid chromatography

High-performance liquid chromatography (HPLC) was used to determine the absolute molecular weight of the RP samples. A Wyatt *Sec*-Mals instrument was used with a Dawn Heleos-II laser detector, Optilab rex refractive index detector, and Shodex Ohpak SB-806 HQ chromatographic column. We used 0.1 M sodium sulfate with 0.2% sodium azide as the mobile phase, with a flow rate of 0.5 mL/min. The sample was injected at a concentration of ~2 mg/mL, with an injection volume of 500 μL, and analysis time of 35 min. Dextran 40,000 (Sinopharm, China) was used as the reference substance for normalization to avoid the need to measure a standard curve. Finally, the absolute molecular weight of RP was calculated according to the principle of light scattering.

2.6. Preparation of microcapsules

An analytical balance was used to precisely weigh 5 samples of 0.15 g of MCE, 0.0375 g of pre-cultured *Lactobacillus plantarum* solution, and 0.0375 g of nisin, which were added to 10 g of distilled water and stirred well. Then, 10, 20, 30, 40, and 50 g of corn oil were added to five separate beakers, and one sample of the mixed aqueous solution was added to each beaker. The mixtures were homogenized for 2 min at 12000 rpm, followed by the addition of 0.3 g of Span 80. Then, a magnetic force blender was added to the mixture. Then, the mixture was poured into a separation funnel and left to stratify. The mass of the aqueous filtrate solution from the lower part of the funnel was measured to calculated the encapsulation efficiency of the W/O microcapsules. Each sample group was tested three times, and the average was calculated. The encapsulation efficiency (ω) of the W/O microcapsules was calculated using the following formula:

$$\omega\,(\%) = (1 - \frac{m_1}{m_0}) \times 100 \tag{2}$$

Here, m_0 is the total mass of the water phase before encapsulation, and m_1 is the total mass of the remaining water phase after encapsulation.

Then, a group of W/O microcapsules with the highest ω was used for re-encapsulation, i.e., the preparation of water-in-oil-in-water (W/O/W) double emulsions. First, an RP solution was prepared by adding ultrapure water (preheated to 40 °C) to the extracted RP powder at a concentration of 1 g/100 mL. The pH of the solution was adjusted to 8.0 with 1 mol/L $NaHCO_3$, and then stirred in a water incubator at 40 °C for 30 min to completely dissolve the RP. After preparing the RP solution, 5 g/100 mL of the prepared W/O microcapsules was slowly added, and then the solution was homogenized at 12000 rpm for 2 min, followed by the slow addition of the prepared 1% (w/v) GA. After the solution was magnetically stirred in a water bath at 25 °C for 5 min, the pH of the solution was adjusted to 3.8 with 1 mol/L citric acid, and then magnetically stirred in a water bath at 25 °C for 15 min to initiate the compound reaction between the RP and GA to prepare W/O/W double emulsions. Five different W/O/W samples were prepared using RP and 1% (w/v) GA solutions with volume ratios of 3:1, 2:1, 1:1, 1:2, and 1:3. In addition, a group with a RP to GA ratio of 1:1 was prepared without corn oil to investigate the formation of the shell of the microcapsules. Finally, the morphology of the prepared W/O/W double emulsion was observed using a stereo microscope at 40× magnification.

2.7. Dispersion stability and particle size

After the preparation of the W/O/W double emulsions were complete, the samples were allowed to stand for 2 h, and then the milky white part of the system was diluted to 1 wt% with distilled water. A Malvern particle size analyzer (Zetasizer Nano ZS90, Malvern Co., Worcestershire, UK) was used to analyze the particle size and zeta potential of the microcapsules (25 °C). Finally, the group with the smallest particle size was selected as the material for subsequent experiments. Each test was performed thrice.

2.8. Noodle preparation

Noodles were prepared using traditional methods. Pure water (40 g) was added to 100 g of low-gluten flour three times, along with 1, 2, 3, 4, or 5 wt% of the microcapsule mixture (based on the flour weight) and salt (0.35 g). The mixture was mixed thoroughly to prepare dough. Fifty grams of dough was used for subsequent rheological property tests, and finally, a manual flour press was used to form the dough into noodles with a length of 200 ± 50 mm and a width of 5 mm. A dough with 5 wt% microcapsules without Nisin etc. was used as the control group. All noodle samples were placed in preservation boxes at room temperature for later use.

2.9. Dynamic rheological properties of sheeted dough

A Discovery HR-2 rheometer (TA Instruments Inc., USA) was used to analyze all dough samples using dynamic oscillatory measurements. Frequency-sweep measurements were performed in the range of 0.1–10 Hz to determine the storage modulus (G'), loss modulus (G''), and tanδ (G''/G') of the dough as a function of frequency. In addition, creep and recovery tests were performed under a fixed stress of $\tau = 100$ Pa within a strain range equal to the ratio of the stress. A creep phase of 150 s and a recovery phase of 300 s were used.

2.10. Noodle preservation performance

Each group of prepared noodles was evenly placed in a disposable polypropylene plastic box, sealed, and placed in a dark environment at room temperature for preservation. The lid of the box was opened every other day to take photographs of the changes in the shape of the noodles. Samples (~4 g) were taken and mixed with physiological saline at a ratio of 1:9 and stirred for 10 min to fully release all the natural microorganisms contained therein. The solution was diluted to a factor of 10^{-4}, and then coated on a gradient-dilution plate. Finally, the content of microorganisms in the noodles was determined by observing the plates using microscopy.

2.11. Cooking behavior of the noodles

Samples of the noodles (25 ± 1 g) were added to 500 mL of pure water and cooked for 8 min, which was the optimal cooking time, where the noodles were sufficiently cooked and no opaque core remained (Hou, 2010). After the noodles were cooked, they were immediately rinsed in 300 mL of pure water (~15 ℃) for 10 s; this process was repeated twice. A colander was used to drain the rinsed noodles, which were then placed on a clean iron plate. The water on the surface of the noodles was blotted with filter paper and then the noodles were weighed. The water absorption rate (WA) of the noodles was calculated using the following formula:

$$\mathrm{WA}\,(\%) = \frac{(W_2 - W_1)}{W_1} \times 100 \tag{3}$$

Here, W_1 is the weight of the noodles before cooking, and W_2 is the weight of the noodles after cooking.

The water used to cook the noodles was collected in a 500-mL volumetric flask and fresh distilled water was added to achieve a volume of 500 mL. After mixing, a 25-mL aliquot was taken and placed in a 50-mL beaker and weighed. Then, the beaker was placed in an oven at 100 ℃ and heated for 24 h to completely evaporate the water. Then, the beaker and remaining material were weighed to determine the cooking loss (CL) M (%) using the following formula:

$$\mathrm{CL}\,(\%) = \frac{W_3}{W_1} \times 100 \tag{4}$$

Here, W_3 is the total mass of noodle residue from the cooking water, and W_1 is the weight of the noodles before cooking.

2.12. Statistical analysis

All measurements were made in triplicate and the results were expressed as mean ± standard deviation. One-way ANOVA was performed on the data using SPSS 22.0 software (IBM Corp., USA). Significant differences between means were determined using Duncan's multiple range test, and differences were considered statistically significant at $p < 0.05$. Origin Pro 2017 (OriginLab Corporation, Northampton, Massachusetts, USA) was used to draw all the figures.

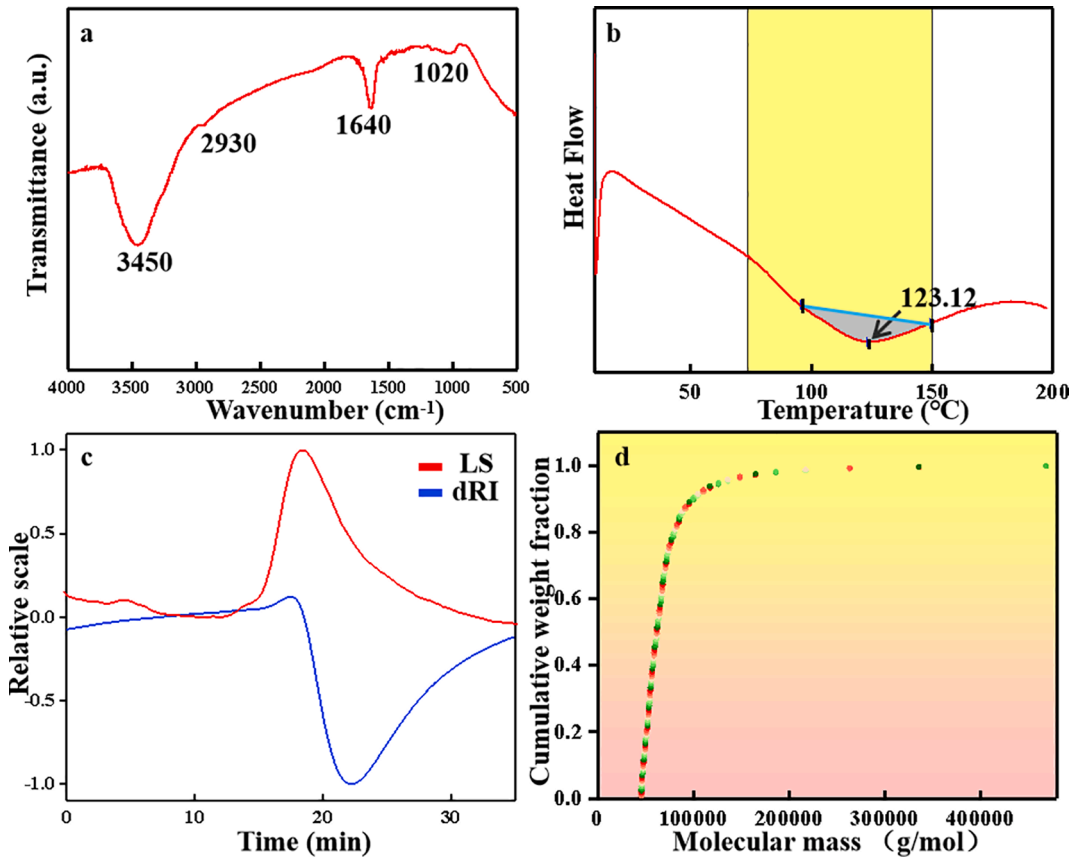

Fig. 1. (a) FTIR spectra; (b) DSC thermograms; (c) chromatograms of RP measured using a laser detector (LS) or differential refractive index detector (dRI); (d) Cumulative weight fraction of RP.

3. Results and discussion

3.1. Protein extraction

Based on the results of the six extractions, the ε of RP for this extraction method was 13.83 ± 1.32%, which was ~5% higher than that of the control group (8.72 ± 1.66%). Yang et al. (2018) found that ultrasonic treatment can increase ε of rice proteins. This is because ultrasonic waves produce cavitation and mechanical effects in the solution, so that the extracted material can move faster, thereby greatly increasing the extraction area. Secondary extraction under microwave treatment was also effective. This is because, under microwave conditions, the forced overheating of trapped water molecules and continuous collisions in the matrix promote the destruction of the cell wall (Flórez, Conde, & Domínguez, 2015), allowing the cell contents to be removed (Kute et al., 2015), thereby further increasing ε. Furthermore, as rock beans mainly contain starch, a relatively low ε of the protein was expected.

3.2. Protein composition

The SDS-PAGE gel electrophoresis pattern of the extracted RP is shown in Fig. S1. The treated RP solution was added to three different channels. Most of the proteins that were easily dissolved in alkaline pH were extracted by alkaline extraction. The figure shows that the RP contained many different subunits in the range of 17–180 kDa, which is similar to the electrophoresis results for soy protein presented by Li, Lin, Bean, Sun, and Wang (2020). In particular, the SDS-PAGE spectrum of RP shows the previously reported soy protein (α-β) subunits at 50–90 kDa (Chen, Zhao, Chassenieux, & Nicolai, 2016), acidic subunits (AS) at 35–40 kDa, and the basic subunits (BS) at 19–22 kDa (Acquah, Zhang, Dubé, & Udenigwe, 2020). In addition, 7S (β-conglycinin) and 11S (glycinin) were the main components of RP, similar to soy protein (Shirotani et al., 2021). The 7S component is composed of three subunits: α' (~71 kDa), α (~67 kDa), and β (~50 kDa). Further, 11S is a hexameric protein composed of five subunits, where each subunit is composed of an acidic subunit A (~35 kDa) and a basic subunit B (~20 kDa), which are connected by S—S bonds (Nishinari, Fang, Guo, & Phillips, 2014). According to previous research, a protein called lipoxygenase with an apparent molecular weight of ~90 kDa was present in pea and soybean proteins (Crévieu et al., 1997). Under reducing conditions, the S—S bonds break, causing the hexameric protein to break down into two subunit peptides (AS and BS) (Shand, Ya, Pietrasik, & Wanasundara, 2007). Here, a weak band at ~90 kDa was observed, indicating that the S—S bonds were not completely destroyed. Therefore, RP may have some resistance to reducing environments, i.e., RP itself may have some reducing properties and could act as an antioxidant, such as Vc. Furthermore, comparing RP with the previously reported soy protein, the electrophoresis band width of the α and β subunits in 7S is much wider, and the width of the α subunit is the same. Therefore, compared with ordinary soy protein, RP contains more β-conglycinin and subunits and is hence expected to have better processing properties, including heat-induced soluble aggregate formation and emulsification ability (Ippoushi, Tanaka, Wakagi, & Hashimoto, 2020).

3.3. RP chemical structure

Fig. 1a shows the FTIR spectrum of RP at 500–4000 cm^{-1}, indicating the distribution of its absorption peaks. In general, the band at 3100–3700 cm^{-1} is attributed to the basic stretching mode of the –OH group (Chakraborty, Valapa, Pugazhenthi, & Katiyar, 2018), while that

around 3450 cm^{-1} is the O—H stretching vibration of RP. The broad band at 2800–3000 cm^{-1} corresponds to the C—H tensile vibration of the triglyceride carbonyl group. The absorption peak at 2930 cm^{-1} is related to the tensile shock of the –C—H (CH_2) group of the few fatty acids in the RP powder. The presence of this band may be a result of insufficient degreasing of the rock-bean flour using the Soxhlet extraction method. The second-highest absorption peak at 1640 cm^{-1} corresponds to the peptide bond (–CO–NH–) related to amide I (ν C═O, ν C—N) reported in the literature. Amide I strongly absorbs infrared light and is highly sensitive to structural changes in the protein amides (Glassford, Byrne, & Kazarian, 2013), while only a weak band was observed for amide II at 1550 cm^{-1} (δ N—H, ν C—N), related to peptide bonds (Andrade et al., 2019). In addition, the absorption band at 1550–1740 cm^{-1} indicates a secondary RP structure (e.g., β-sheet, antiparallel β-sheet, random coil, or α-helix). This is consistent with the SDS-PAGE electrophoresis pattern. The absorption peak around 1020 cm^{-1} represents the polysaccharide region, which is usually related to the extension of C—O bands in carbohydrates (El Darra et al., 2017).

3.4. Thermal stability of RP

The DSC spectrum of RP shown in Fig. 1b provides information about the temperature dependence of the protein, while its thermal stability is characterized by its transition temperature. It is well known that the process of protein denaturation by heat is irreversible, where proteins with higher thermal transition temperature have better thermal stability (Luo et al., 2022). RP showed an endothermic peak in the temperature range of 76.98–149.73 °C, attributed to the removal of adsorbed water (Costa, Miki, Ramos, & Teixeira-Costa, 2020). In addition, the endothermic peak located at 123.12 ℃ was attributed to the denaturation of RP. This is similar to the denaturation temperature of the 7S and 11S globulin components in freeze-dried soy protein reported previously (Li et al., 2020b). Furthermore, although there is only one pronounced endothermic peak in the spectrum, a slight downward trend was observed at ~76.98 °C, indicating the endothermic peak of 7S (Tang, Choi, & Ma, 2007). This weak peak may be due to local transient overheating during ultrasound extraction, which may have denatured the 7S in the protein. The endothermic peak of 11S in the RP is ~30 °C higher than that of the reported soy protein (Khatkar, Kaur, & Khatkar, 2020). The delay in the 11S endothermic peak was attributed to the denaturation of 7S by ultrasonic treatment, which affects the conformation of the protein and destroys the non-covalent bond force of hydrogen bonds. Coupled with ultrasonic cavitation, shear and turbulence cause electrostatic interactions between molecules, resulting in the exposure of internal hydrophobic groups on the molecular surface. These groups form a stable framework through intermolecular interactions, and the partially dissociated protein components are refolded to form more stable aggregates. The subsequent microwave extraction may further contribute to this process. These findings indicate that RP produced by ultrasound/microwave extraction has better thermal stability than soy protein.

3.5. Molecular weight of RP

To determine the molecular weight and distribution of RP, HPLC tests were performed. Fig. 1c shows the HPLC spectra of the RP using a laser detector (LS) and a differential refractive index detector (dRI). Both results showed a single uniform peak, indicating that the extracted RP was a uniform substance. The downward peak of the dRI indicates that the polarity of the RP is opposite to that of the mobile phase. The number-average molecular weight (*Mn*) of RP was 64,430 g/mol, the weight-average molecular weight (*Mw*) was 75,240 g/mol, the higher average molecular weight (*Mz*) was 149,400 g/mol, the highest peak molecular weight (*Mp*) was 67,450 g/mol, and the polydispersity index (*Mw/Mn*) was 1.168. In addition, the peaks of the two curves were quite broad, indicating that the molecular weight distribution range of RP is quite wide. This was consistent with the high *Mw/Mn* value. This differs from monodisperse polymers with equal chain lengths, such as natural proteins, that usually have $Mw/Mn = 1$. This result may be related to the ultrasonic extraction process, because the polydispersity index depends on the mechanical dissociation strength, where ultrasonic treatment provides a higher shear force than standard mechanical methods. However, the *Mw/Mn* of soy protein was close to 1. This may be related to the denaturation of 7S during ultrasound and the formation of new aggregates due to electrostatic interactions. This result is consistent with the weak 7S peak observed in DSC. Fig. 1d shows the cumulative weight fraction versus molecular weight, which allows an easy comparison of the differences in molecular weight and distribution between samples, i.e., the percentage distribution of the molecular weight. The distribution can be classified into three parts, and the separation between them is not absolute: 45,500–72,000, 72,000–140,000, 140,000–470,000, and 758,000 g/mol. The molecular weight of RP was mostly concentrated in the range of 45,500–72,000 g/mol, accounting for 70.4% of the total, while the 72,000–140,000 and 140,000–470,000 g/mol regions only accounted for 25.4% and 4.2%, respectively. This is consistent with the results obtained by electrophoresis, and further proves that the RP contained large amounts of 7S and 11S, and a small amount of lipoxygenase.

Table 1
Encapsulation efficiency of W/O microcapsules with different oil–water ratios; zeta potential and particle size of W/O/W double emulsions with different RP/GA ratios.

Oil-water ratio	Encapsulation efficiency (%)	RP: GA	Zeta potential (mV)	Particle size (nm)
1:1	9.06 ± 0.19^{e}	3:1	-20.17 ± 0.67^{a}	7896.67 ± 381.12^{a}
2:1	17.12 ± 0.26^{d}	2:1	-22.37 ± 0.38^{ab}	5345 ± 368.21^{b}
3:1	19.63 ± 0.47^{c}	1:1	-27.17 ± 7.84^{ab}	1852.67 ± 148.53^{e}
4:1	20.87 ± 0.46^{b}	1:2	-22.97 ± 0.49^{ab}	2730 ± 575.86^{d}
5:1	28.21 ± 0.34^{a}	1:3	-30.70 ± 6.67^{b}	3751.67 ± 715.51^{c}

Different letters in the same column indicate significant differences ($p < 0.05$).

3.6. W/O/W double emulsions

The ω of the as-prepared W/O microcapsules for nisin, *Lactobacillus plantarum*, and MCE mixtures is shown in Table 1. For a fixed homogeneity strength and Span 80 content, as the amount of added corn oil increased, the ω of the W/O microcapsules for the active substance increased. When the ratio of corn oil to water was 5:1, ω reached 28 ± 0.34%, which is ~20% higher than that of the 1:1 group. However, this does not indicate that the oil phase used for encapsulation reached saturation. The morphology of the W/O microgel observed using stereo microscopy is shown in Fig. S2. Fig. S2 a2-e2 represents the morphology of W/O microcapsules at different ratios of 1:1–5:1. The 2:1 oil–water ratio produced W/O microcapsules with the most uniform size and shape (Fig. S2 b2) of all ratios. However, the ω of this sample was only 17.12%, probably because, as the oil-phase ratio increases, the coverage area of the oil relative to the water phase increases under the action of high-speed shear homogenization. However, after homogenization, the scope of action of the emulsifier increased. Therefore, the encapsulation capacity of the limited oil phase was limited. The morphological stability of the microcapsules was enhanced in the presence of the Span 80 emulsifier. The dissolution of MCE resulted in a brown solution, where obvious encapsulation phenomena can be seen in each image picture. The morphology of the W/O/W double emulsions after the second encapsulation is shown in Fig. S2a1-e1. First, Fig. S2A shows the formation of a microcapsule shell without the addition of corn oil. According to previous studies, GA can form a relatively stable coacervate

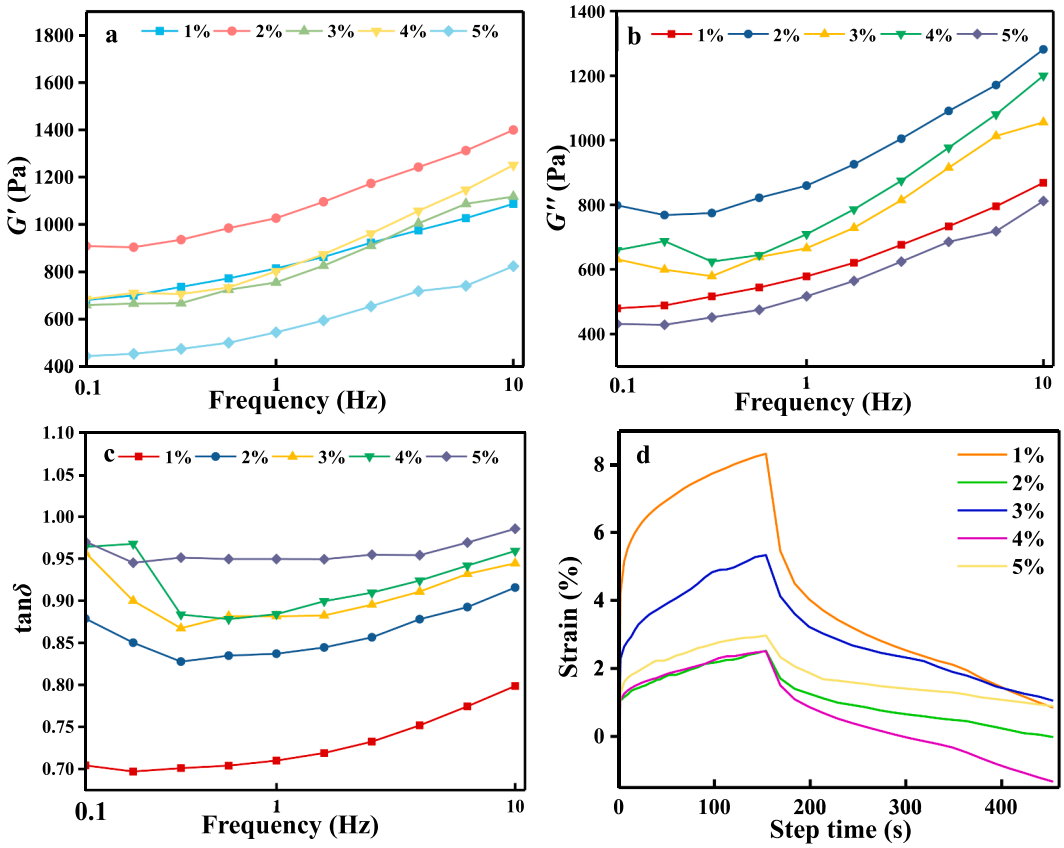

Fig. 2. Rheological properties of doughs with different W/O/W double emulsion concentrations. a) G′, b) *G″*, and c) tan *δ* curves as a function of frequency; d) greep–recovery curves.

with proteins via electrostatic interactions (Eratte et al., 2015). In the RP/GA system without corn oil, an irregular complex was formed that was prone to fragmentation and agglomeration (Plati, Ritzoulis, Pavlidou, & Paraskevopoulou, 2021). After adding the W/O microcapsules, highly spherical structures were formed, with the RP/GA complex dispersed as a surface layer to achieve encapsulation. In the case of RP/GA ratios of 3:1 and 2:1, both encapsulated microcapsules and unembedded complex aggregates were observed. When the GA content was increased (RP/GA ratios of 1:2 and 1:3), a thinner complex coacervate was observed, along with some non-spherical microcapsules. This could be due to the following reasons. According to a previous report, all proteins tend to form aggregates under the action of aggregation kinetics (Medina & Candia, 2021). When a large fraction of RP is added, some of the proteins form a complex with GA through electrostatic interactions, while the remainder self-aggregates. For lower RP fractions, fewer complexes were formed in the system. In addition, when the pH is close to its isoelectric point, the emulsification ability of the protein may deteriorate due to the decrease in the electrostatic repulsion force (Taktak et al., 2019), which is exacerbated by reducing the amount of protein, resulting in smaller microcapsules.

3.7. Zeta potential and particle size

The zeta potential and particle size of the samples were analyzed to determine the gravitational stability and average particle size of the microcapsules in solution. The zeta potential of the microcapsules was between 20.17 and 30.70 mV (Table 1). According to related reports, such high absolute zeta potential values indicate that the particles have good electrical stability, which prevents self-aggregation and flocculation, resulting in high dispersibility and gravitational stability (Medina, Tamm, Guadix, Guadix, & Drusch, 2016). Although RP and GA formed many complexes at ratios of 3:1 and 2:1, the presence of these complexes may be similar to the results shown in Fig. S2A without W/O microcapsules, indicating that these complexes could be better dispersed in solution. Considering both the particle size results and the microstructures shown in Fig. S2, the particle size tends to first decrease and then increase with increasing ratio of RP/GA. However, in Fig. S2, the particle size shown a decreasing result. This could be because, when the RP/GA ratio was high, the two formed more complex aggregates, which influenced the particle-size analysis. When the RP/GA ratio was low, the insufficient RP content reduced the emulsifying ability of the system, resulting in an unstable complex. Further, when the protein is close to the isoelectric point, the electrostatic repulsive forces are weak, further reducing the emulsifying ability of the protein. Considering these results, an RP/GA ratio of 1:1 was considered the optimal ratio to form the shell of W/O/W double emulsions.

3.8. Rheological properties of dough with added microcapsules

Figss. 2a-c show changes in the G′, G″, and tan *δ* curves, respectively, as a function of frequency for the dough samples with different microcapsule concentrations. During dough preparation, a hydrated gluten network is formed, which changes the viscoelastic properties of the dough (Sofou, Muliawan, Hatzikiriakos, & Mitsoulis, 2008). The G′ and G″ curves showed a consistent trend overall. The dough with 2% microcapsules had the largest G′ and G″, while the values for the 3% and 4% doughs were similar to those of the 1% sample. It is proposed that a 2% microcapsule concentration provided optimal contact with the hydrophilic protein in the flour, resulting in an increase in volume that is conducive to the formation of a high-quality gluten network, thereby strengthening the overall flexibility of the dough. At 1% microcapsule concentration, there may be insufficient water for gluten formation,

Table 2
Cooking characteristics of noodles with different microcapsule concentrations.

Addition of microcapsules (%)	Water absorption (%)	Cooking loss (%)	Noodle soup absorbance value (670 nm)
0	49.76 ± 5.51^{bc}	1.89 ± 0.45^{d}	0.083 ± 0.002^{d}
1	47.43 ± 0.57^{c}	2.07 ± 0.25^{cd}	0.081 ± 0.002^{e}
2	49.87 ± 0.62^{bc}	2.23 ± 0.26^{cd}	0.093 ± 0.001^{c}
3	57.12 ± 2.22^{a}	2.47 ± 0.24^{bc}	0.096 ± 0.001^{b}
4	55.20 ± 2.15^{ab}	2.76 ± 0.04^{ab}	0.099 ± 0.002^{b}
5	55.38 ± 6.61^{ab}	3.12 ± 0.06^{a}	0.101 ± 0.001^{a}

resulting in lower moduli. When the microcapsule concentration exceeds 2%, the moisture content of the dough increases excessively, which increases the mobility between protein chains in the gluten network (Sandeep & Narpinder, 2013), thereby reducing the moduli. This result is also confirmed in the change of tan δ with increasing microcapsule concentration. The increase of tan δ in the range of <1, indicates that the increase in the amount of microcapsules resulted in the dough transforming to a semi-solid material. Fig. 2d shows the creep–recovery curves of the doughs. In the creep phase, the strain of the sample increased continuously over time. In the recovery step, the amount of deformation gradually recovered and stabilized as the external force continued to decrease. The dough with 2% microcapsules showed the best experimental results.

3.9. Effects of microcapsule addition on noodle cooking behavior

The water absorption and cooking loss rates are important indicators of the cooking behavior of noodles, which is closely related to a customer's perception of the quality of the product. Table 2 shows the water absorption and cooking loss rates of noodles with different microcapsule concentrations. The cooking loss represents the total dry content of noodles dissolved in the water during the cooking process. The scattering of the soluble components of the noodles increases the turbidity of the cooking water due to the leaching of amylose in the noodles and the solubilization of some salt-soluble proteins (Zhu et al., 2013). This reflects how closely the various ingredients in cooked noodles are combined. The cooking loss rate of the noodles with added microcapsules showed an increasing trend, reaching a maximum at 5 wt% microcapsules, which is about 1.2% higher than that of the control group, indicating that more binding components were dispersed during cooking. This may a result of the water from the microcapsule reducing the strength of gluten, which is exacerbated during cooking (Luo et al., 2022). In addition, during cooking, denaturation of the RP by heat can damage the outer shell of the microcapsule, resulting in the release of the internal oily components, thereby reducing the connection between hydrophilic components and damaging the noodle structure. In general, the water absorption rate of the different noodles first increased and then stabilized. This is in contrast to the cooking loss of the noodles. It has been reported that the water absorption rate of noodles decreases with an increase in cooking loss. This may be due to the increase in the amount of added microcapsules, which increases the protein content in the dough, which can bind more water. The absorbance at 670 nm of the noodle cooking water is shown in Table 2. The change in absorbance was consistent with the cooking loss trend as a function of microcapsule concentration.

3.10. Noodle preservation

The growth of microorganisms is dependent on the temperature, moisture content, and nutrients in the environment. Microorganisms can grow quickly when the conditions are suitable, and freshly made noodles meet these conditions. In addition, during the storage of noodles, the loss of water and the decrease in pH also affect the growth of microorganisms. When the pH is <6.5, fungi start to compete with bacteria. When the pH reaches 4.5, fungi have the advantage in the culture. The common molds found on food products are fungi. Fig. 3 shows the changes in the surface morphology of the noodles. The color of all groups of noodles became darker over time, probably due to the development of polyphenol oxidase, which is a key factor that causes noodles to change color. In all groups of noodles, obvious mycelia appeared on the day 5, and there were obvious plaques on the surfaces of the groups with 0% and 1% microcapsules.

According to the petri-dish results (Fig. 4), these two groups already contained a large number of microbial flora on the third day. The changes in the number of colonies showed that the microbial flora was dominated by bacteria. Later, due to its own metabolism and accumulation of substances, the pH value of the noodles decreased, which was not conducive to the growth of bacteria, resulting in the dominance of mold. By the fifth day, characteristic colonies of mold appeared on the 0% and 1% noodles. Compared with the control group, the noodles with microcapsules delayed the appearance of mold. These results indicate that the pH of the 0% group dropped the fastest, and the microbes may have started explosive growth on day 4. Compared with the 0% and 1% groups, the number of microorganisms in the other groups was much smaller, which indicates that the nisin contained in the microcapsules had an inhibitory effect on the microorganisms, although the effect was not obvious for small concentrations. When the microcapsule content was too high, it contributed significantly to increasing the water content in the noodles, which facilitated the growth of microorganisms. Typical fresh noodles have a shelf life of only 1–2 d under normal conditions, and they are not suitable for consumption afterwards. The addition of microcapsules to the noodles can extend the shelf life by 1–2 d, where

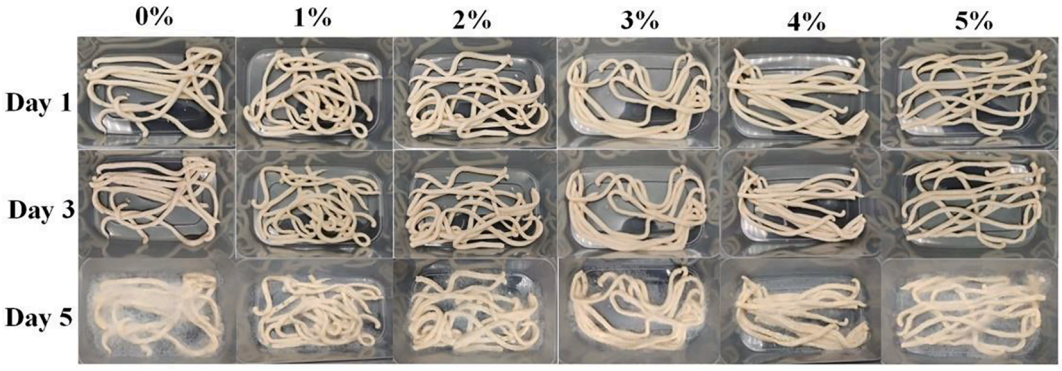

Fig. 3. Changes in the appearance of noodles during storage.

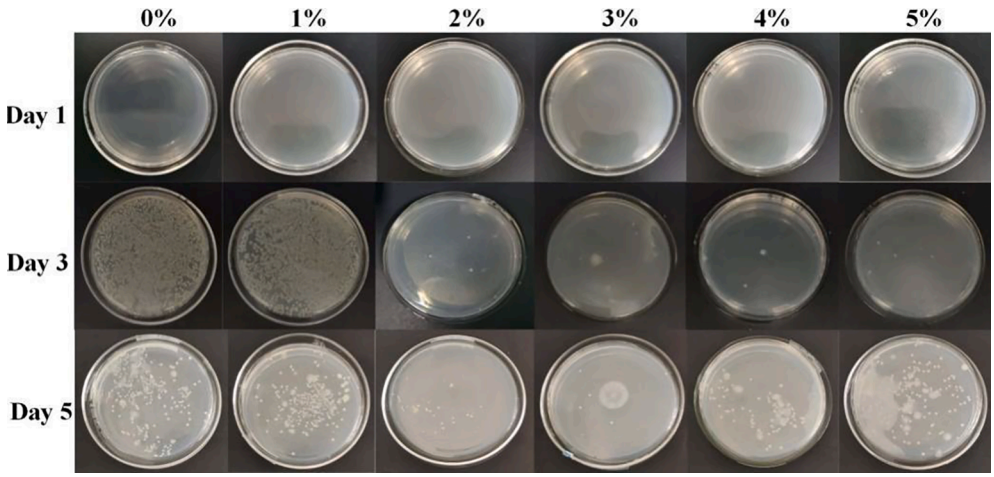

Fig. 4. Changes in the number of colonies and types of microorganisms on the noodles during storage.

2–3% of the additive showed optimal results. The petri-dish results suggested that the addition of 3% microcapsules had a better preservation effect than the 2% group.

4. Conclusion

Ultrasonic treatment and microwave extraction were used to increase the protein extraction rate of RP from wild rock beans. Characterization of the extracted RP showed that it contains high amounts of 7S and 11S globulin, and has good thermal stability and potential antioxidant properties. W/O/W double emulsions were prepared by high-speed shear homogenization of RP and GA, where RP formed a stable coacervate with GA through electrostatic interactions and provided a good encapsulation effect. Optimal microcapsules were produced with a 1:1 RP/GA ratio and a corn-oil/water ratio of 5:1. The addition of 2 wt% microcapsules to low-gluten flour resulted in dough with suitable rheological properties and optimal cooking loss and water absorption when used to produce noodles. Noodle preservation experiments showed that the addition of nisin via the microcapsules extended the shelf life of the fresh noodles, where the addition of 3 wt% microcapsules had the best effect in delaying the growth of bacteria and mold. The findings of this study demonstrate that microcapsule technology can be successfully applied to wheat dough to develop new noodle products with, e.g., enhanced nutrition, longer storage life, and better cooking performance.

Declaration of Competing Interest

The authors declare that they have no known competing financial interests or personal relationships that could have appeared to influence the work reported in this paper.

Acknowledgments

This work was supported by Sichuan Science and Technology Program (2019YFN0174, 2020YFN0149 and 2021JDRC0033).

References

Acquah, C., Zhang, Y., Dubé, M. A., & Udenigwe, C. C. (2020). Formation and characterization of protein-based films from yellow pea (Pisum sativum) protein isolate and concentrate for edible applications. *Current Research in Food Science, 2*, 61–69.

Andrade, O., Pereira, C. G., Junior, J. C. D. A., Viana, C. C. R., Neves, L. N. D. O., Silva, P. H. F. D., et al. (2019). FTIR-ATR determination of protein content to evaluate whey protein concentrate adulteration. *LWT, 99*, 166–172.

Chakraborty, G., Valapa, R. B., Pugazhenthi, G., & Katiyar, V. (2018). Investigating the properties of poly (lactic acid)/exfoliated graphene based nanocomposites fabricated by versatile coating approach. *International Journal of Biological Macromolecules, 113*, 1080–1091.

Chen, N., Zhao, M., Chassenieux, C., & Nicolai, T. (2016). Data on the characterization of native soy globulin by SDS-Page, light scattering and titration. *Data in Brief, 9*, 749–752.

Costa, J. C. M. D., Miki, K. S. L., Ramos, A. D. S., & Teixeira-Costa, B. E. (2020). Development of biodegradable films based on purple yam starch/chitosan for food application. *Heliyon, 6*(4), e03718.

Crévieu, I., Carré, B., Chagneua, A. M., Quillien, L., Guéguen, J., & Bérot, S. (1997). Identification of resistant pea (*Pisum sativum L.*) proteins in the digestive tract of chickens. *Journal of Agricultural and Food Chemistry, 45*, 1295–1300.

Dillon, V., & Board, R. (1994). Natural antimicrobial systems and food preservation. *Journal of Food Safety, 16*, 239–241.

El Darra, N., Rajha, H. N., Saleh, F., Al-Oweini, R., Maroun, R. G., & Louka, N. (2017). Food fraud detection in commercial pomegranate molasses syrups by UV–VIS spectroscopy, ATR-FTIR spectroscopy and HPLC methods. *Food Control, 78*, 132–137.

Eratte, D., McKnight, S., Gengenbach, T. R., Dowling, K., Barrow, C. J., & Adhikari, B. P. (2015). Co-encapsulation and characterisation of omega-3 fatty acids and probiotic bacteria in whey protein isolate–gum Arabic complex coacervates. *Journal of Functional Foods, 19*, 882–892.

Flórez, N., Conde, E., & Domínguez, H. (2015). Microwave assisted water extraction of plant compounds. *Journal of Chemical Technology & Biotechnology, 90*(4), 590–607.

Glassford, S. E., Byrne, B., & Kazarian, S. G. (2013). Recent applications of ATR FTIR spectroscopy and imaging to proteins. *Biochimica et Biophysica Acta (BBA) – Proteins and Proteomics, 1834*(12), 2849–2858.

Gong, F., Qian, J., Chen, Y., Yao, S., Tong, J., & Guo, H. (2018). Preparation and properties of gum arabic cross-link binding nisin microparticles. *Carbohydrate Polymers, 197*, 608–613.

Hou, & Gary, G. (2010). Laboratory pilot-scale asian noodle manufacturing and evaluation protocols. *John Wiley & Sons, Inc.* 183-225.

Ippoushi, K., Tanaka, Y., Wakagi, M., & Hashimoto, N. (2020). Evaluation of protein extraction methods for β-conglycinin quantification in soybeans and soybean products. *LWT, 132*, Article 109871.

Khatkar, A. B., Kaur, A., & Khatkar, S. K. (2020). Restructuring of soy protein employing ultrasound: Effect on hydration, gelation, thermal, in-vitro protein digestibility and structural attributes. *LWT, 132*, Article 109781.

Le, B., & Yang, S. H. (2018). Efficacy of Lactobacillus plantarum in prevention of inflammatory bowel disease. *Toxicology Reports, 5*, 314–317.

Li, J., Lin, H., Bean, S. R., Sun, X. S., & Wang, D. (2020a). Evaluation of adhesive performance of a mixture of soy, sorghum and canola proteins. *Industrial Crops and Products, 157*, Article 112898.

Li, D., Liu, B., Yang, F., Wang, X., Shen, H., & Wu, D. (2016). Preparation of uniform starch microcapsules by premix membrane emulsion for controlled release of avermectin. *Carbohydrate Polymers, 136*, 341–349.

Li, D., Wu, G., Zhang, H., & Qi, X. (2020b). The soy protein isolate-Octacosanol-polysaccharides nanocomplex for enhanced physical stability in neutral conditions: Fabrication, characterization, thermal stability. *Food Chemistry, 322*, Article 126638.

Liu, Y., Sameen, E. D., Ahmed, S., Dai, J., & Qin, W. (2021). Antimicrobial peptides and their application in food packaging. *Trends in Food Science & Technology, 112*, 471–483.

Luo, S., Chen, J., He, J., Li, H., Jia, Q., Hossen, M. A., et al. (2022a). Preparation of corn starch/rock bean protein edible film loaded with d-limonene particles and their application in glutinous rice cake preservation. *International Journal of Biological Macromolecules, 206*, 313–324.

Luo, Q., Hossen, M. A., Zeng, Y., Dai, J., Li, S., Qin, W., et al. (2022b). Gelatin-based composite films and their application in food packaging: A review. *Journal of Food Engineering, 313*, Article 110762.

Medina, A. G., & Candia, C. N. H. (2021). Aggregation kinetics of the protein photoreceptor Vivid. *Biochimica et Biophysica Acta (BBA) – Proteins and Proteomics, 1869*(5), Article 140620.

Medina, R. M., Tamm, F., Guadix, A. M., Guadix, E. M., & Drusch, S. (2016). Functional and antioxidant properties of hydrolysates of sardine (S. pilchardus) and horse mackerel (T. mediterraneus) for the microencapsulation of fish oil by spray-drying. *Food Chemistry, 194*, 1208–1216.

Nishinari, K., Fang, Y., Guo, S., & Phillips, G. O. (2014). Soy proteins: A review on composition, aggregation and emulsification. *Food Hydrocolloids, 39*, 301–318.

Nualkaekul, S., Lenton, D., Cook, M. T., Khutoryanskiy, V. V., & Charalampopoulos, D. (2012). Chitosan coated alginate beads for the survival of microencapsulated Lactobacillus plantarum in pomegranate juice. *Carbohydrate Polymers, 90*(3), 1281–1287.

Plati, F., Ritzoulis, C., Pavlidou, E., & Paraskevopoulou, A. (2021). Complex coacervate formation between hemp protein isolate and gum Arabic: Formulation and characterization. *International Journal of Biological Macromolecules, 182*, 144–153.

Sandeep, S., & Narpinder, S. (2013). Relationship of polymeric proteins and empirical dough rheology with dynamic rheology of dough and gluten from different wheat varieties. *Food Hydrocolloids, 33*(2), 342–348.

Shand, P. J., Ya, H., Pietrasik, Z., & Wanasundara, P. K. J. P. D. (2007). Physicochemical and textural properties of heat-induced pea protein isolate gels. *Food Chemistry, 102*(4), 1119–1130.

Shirotani, N., Hougaard, A. B., Lametsch, R., Petersen, M. A., Rattray, F. P., & Ipsen, R. (2021). Proteolytic activity of selected commercial Lactobacillus helveticus strains on soy protein isolates. *Food Chemistry, 340*, Article 128152.

Sofou, S., Muliawan, E. B., Hatzikiriakos, S. G., & Mitsoulis, E. (2008). Rheological characterization and constitutive modeling of bread dough. *Rheologica Acta, 47*(4), 369–381.

Sun, Z., Sun, K., Zhang, H., Liu, H., Wu, D., & Wang, X. (2021a). Development of poly (ethylene glycol)/silica phase-change microcapsules with well-defined core-shell structure for reliable and durable heat energy storage. *Solar Energy Materials and Solar Cells, 225*, Article 111069.

Sun, H., Zhang, M., Liu, Y., Wang, Y., Chen, Y., Guan, W., et al. (2021b). Improved viability of Lactobacillus plantarum embedded in whey protein concentrate/pullulan/trehalose hydrogel during freeze drying. *Carbohydrate Polymers, 260*, Article 117843.

Taktak, W., Nasri, R., Lopez-Rubio, A., Hamdi, M., Gomez-Mascaraque, L. G., Amor, N. B., et al. (2019). Improved antioxidant activity and oxidative stability of spray dried European eel (*Anguilla anguilla*) oil microcapsules: Effect of emulsification process and eel protein isolate concentration. *Materials Science and Engineering: C, 104*, Article 109867.

Tang, C., Choi, S., & Ma, C. (2007). Study of thermal properties and heat-induced denaturation and aggregation of soy proteins by modulated differential scanning calorimetry. *International Journal of Biological Macromolecules, 40*(2), 96–104.

Taylor, L. (2002). Herbal secrets of the rainforest Technical data report for bitter melon (*Momordica charantia*). *NSW Public Health Bulletin, 13*(4), 1–124.

Wee, S. M., Loud, D. E., Tan, V. W. K., & Forde, C. G. (2019). Physical and sensory characterisation of noodles with added native and denatured pea protein isolate. *Food Chemistry, 294*, 152–159.

Yang, X., Li, Y., Li, S., Oladejo, A. O., Wang, Y., Huang, S., et al. (2018). Effects of ultrasound-assisted α-amylase degradation treatment with multiple modes on the extraction of rice protein. *Ultrasonics Sonochemistry, 40*, 890–899.

Zhang, R., Lan, W., Ji, T., Sameen, E. D., Ahmed, S., Qin, W., et al. (2021). Development of polylactic acid/ZnO composite membranes prepared by ultrasonication and electrospinning for food packaging. *LWT – Food Science and Technology, 135*, Article 110072.

Zhu, K., Li, J., Li, M., Guo, X., Peng, W., & Zhou, H. (2013). Functional properties of chitosan–xylose Maillard reaction products and their application to semi-dried noodle. *Carbohydrate Polymers, 92*(2), 1972–1977.